Structural Engineering and Mechanics, *Vol. 61, No. 1 (2017) 65-76*
DOI: https://doi.org/10.12989/sem.2017.61.1.065

In-plane and out-of-plane waves in nanoplates immersed in bidirectional magnetic fields

Keivan Kiani[*1], Saeed Asil Gharebaghi[1a] and Bahman Mehri[2b]

[1]*Department of Civil Engineering, K.N. Toosi University of Technology, Tehran, Iran*
[2]*Department of Mathematical Sciences, Sharif University of Technology, Tehran, Iran*

(Received April 4, 2016, Revised July 24, 2016, Accepted September 7, 2016)

Abstract. Prediction of the characteristics of both in-plane and out-of-plane elastic waves within conducting nanoplates in the presence of bidirectionally in-plane magnetic fields is of interest. Using Lorentz's formulas and nonlocal continuum theory of Eringen, the nonlocal elastic version of the equations of motion is obtained. The frequencies as well as the corresponding phase and group velocities pertinent to the in-plane and out-of-plane waves are analytically evaluated. The roles of the strength of in-plane magnetic field, wavenumber, wave direction, nanoplate's thickness, and small-scale parameter on characteristics of waves are discussed. The obtained results show that the in-plane frequencies commonly grow with the in-plane magnetic field. However, the transmissibility of the out-of-plane waves rigorously depends on the magnetic field strength, direction of the propagated transverse waves, small-scale parameter, and thickness of the nanoplate. The criterion for safe transferring of the out-of-plane waves through the conducting nanoplate immersed in a bidirectional magnetic field is also explained and discussed.

Keywords: conducting nanoplate; in-plane and out-of-plane waves; bidirectional magnetic field; Nonlocal Kirchhoff plate theory

1. Introduction

Generally, nanoplates are synthesized nano-objects whose two dimensions are considerably larger than another one. Scientists are still working on their usages in various branches of technology and industry. Several potential applications of nanoplates such as electrocatalyst (Chen, Lim *et al*. 2009, Lee, Chiou *et al*. 2011, Huang, Chen *et al*. 2012), biosensor (Abouzar, Poghossian *et al*. 2011, Zhong, Gan *et al*. 2013, Fatemi, Khodadadi *et al*. 2012), corrosion and wear resistance soft magnets (Zhu, Zhao *et al*. 2012, Grzelczak, Perez-Juste *et al*. 2008, Huang and Wang 2011), recording heads and soft magnetic disk drive components subjected to wear (Clark, Wood *et al*. 1997) as well as computer hard drive platen (Sewell 2008) have been of concern of researchers during the recent years. For each application, the deformation regime of the nanoplate should be also rationally examined via appropriate models. For example, the later application of the nanoplates requires true understanding of their dynamic behavior as well as the mechanisms of wave propagation within them in the presence of a magnetic field. This matter motivated the author to study this problem for elastic nanoplates in the presence of an in-plane steady magnetic field.

When a conducting nanoplate is subjected to a magnetic field, a body force is exerted on each element of the nanoplate, called Lorentz's force. Such a force is calculated based on the Lorentz formula and Maxwell's equations. Such a force is commonly expressed as a function of derivatives of deformation and it appears as a body force in the governing equations. Thereby, vibration behavior of conducting nanoplates is affected by the applied magnetic field. It is also indicated that the characteristics of the propagated waves within conducting nanostructures can be appropriately controlled by proper application of the magnetic field. For instance, it has been shown that the transverse stiffness of carbon nanotubes is enhanced by application of a longitudinal magnetic field (Kiani 2012a, Kiani 2014a, Murmu, McCarthy *et al*. 2012, 2013, Karlicic, Murmu *et al*. 2014).

The classical continuum theory (CCT) fails in predicting the true in-plane and out-of-plane vibrations of nanoplates since it does not take into account interatomic forces in its formulations. According to the CCT, the state of stress of each point of the continuum only depends on the state of strain of that point. This matter becomes a serious problem in capturing the characteristics of propagated sound waves when their wavelengths are comparable with the atomic bond length. To overcome such a malfunctioning of the classical continuum theory, some advanced elasticity theories have been developed during the past century such as couple stress theory by Cosserat and Cosserat (1909), generalized couple stress theory by Toupin (1964) and Mindlin (1964), nonlocal continuum theory by Eringen and Edelen (1972), Eringen (1972), Eringen (1983), and strain gradient theory of elasticity by Aifantis (1992). Among the above-mentioned advanced theories, the nonlocal continuum theory (NCT) of Eringen has gained much popularity in various scientific and technical communities.

*Corresponding author, Assistant Professor
E-mail: k_kiani@kntu.ac.ir; keivankiani@yahoo.com
[a]Assistant Professor, E-mail: asil@kntu.ac.ir
[b]Professor, E-mail: mehri@sharif.edu

http://www.techno-press.org/?journal=sem&subpage=8
ISSN: 1225-4568 (Print), 1598-6217 (Online)

This fact is mainly related to its effectiveness in predicting vibration behavior of nanoscale structures as well as its simplicity in application to the classical version of the equations of motion of the continuum under study. Simply, the NCT states that the stress of each point of the equivalent continuum structure pertinent to the nanostructure does not only rely on the stress of that point, but also to the stresses of its neighboring points. Thereby, it could be directly concluded that the discrepancies between the predicted results by the CCT and those of the NCT increase as the frequency of the propagated wave increases.

To date, vibrations of nanoplates have been investigated using nonlocal continuum theory of Eringen for a wide range of problems including free transverse vibration (Pradhan and Phadikar 2009, Malekzadeh and Setoodeh 2011, Jomehzadeh and Saidi 2011, Asadi and Farshi 2010, Ansari, Rajabiehfard *et al*. 2010, Ansari, Arash *et al*. 2011, Ansari, Sahmani *et al*. 2010, Ansari, Shahabodini *et al*. 2015), free in-plane vibration (Murmu and Pradhan 2009), forced transverse vibration (Aksencer and Aydogdu 2012, Malekzadeh and Farajpour 2012, Assadi 2013), and in-plane and out-of-plane vibrations due to moving nanoparticles (Kiani 2011a, b). Concerning the influence of magnetic field on dynamic behavior of nanostructures, there are some works that explain the effect of magnetic fields on vibrations of- and wave propagation in carbon nanotubes (Wang, Dong *et al*. 2010, Wang, Shen *et al*. 2012, Xie, Wang *et al*. 2012, Narendar, Gupta *et al*. 2012, Kiani 2014b, c) and nanowires (Kiani 2012b, c). In the first six works, the applied magnetic field is steady whereas in the latter two ones, the magnetic field is unsteady and considering the inertial effects of the nanostructure leads to a more rational dynamic response. Additionally, free transverse vibrations of magnetically affected graphene sheets via nonlocal Kirchhoff plate theory (Murmu, McCarthy *et al*. 2013, Kiani 2014d, Li , Cai *et al*. 2014, Mandal and Pradhan 2014, Ke, Wang *et al*. 2014) and vibration behavior of nanoplates via nonlocal shear deformable plate theories (Kiani 2014e, Ansari and Gholami 2016) have been investigated. In these studies, the nanoplates were subjected to unidirectional magnetic fields, their in-plane vibration was provoked, and the characteristics of elastic waves within magnetically affected nanoplates were not addressed. In order to bridge these scientific gaps, the authors were encouraged to revisit the problem in a more general context, namely *in-plane and out-of-plane waves in nanoplates immersed in bidirectional in-plane magnetic fields*.

In the present work, sound wave propagation within conducting nanoplates subjected to biaxially in-plane steady magnetic fields is of concern. By exploiting the nonlocal continuum theory of Eringen, the governing equations of the problem are constructed according to the Lorentz's body force and Maxwell's equations. For a harmonic wave with an arbitrarily propagated direction, the frequencies as well as phase and group velocities of both in-plane and out-of-plane waves within an infinite conducting nanoplate are analytically calculated. The effects of the in-plane magnetic field strength, direction of wave propagation, and wavenumber on the characteristics of the propagated waves are addressed in some detail.

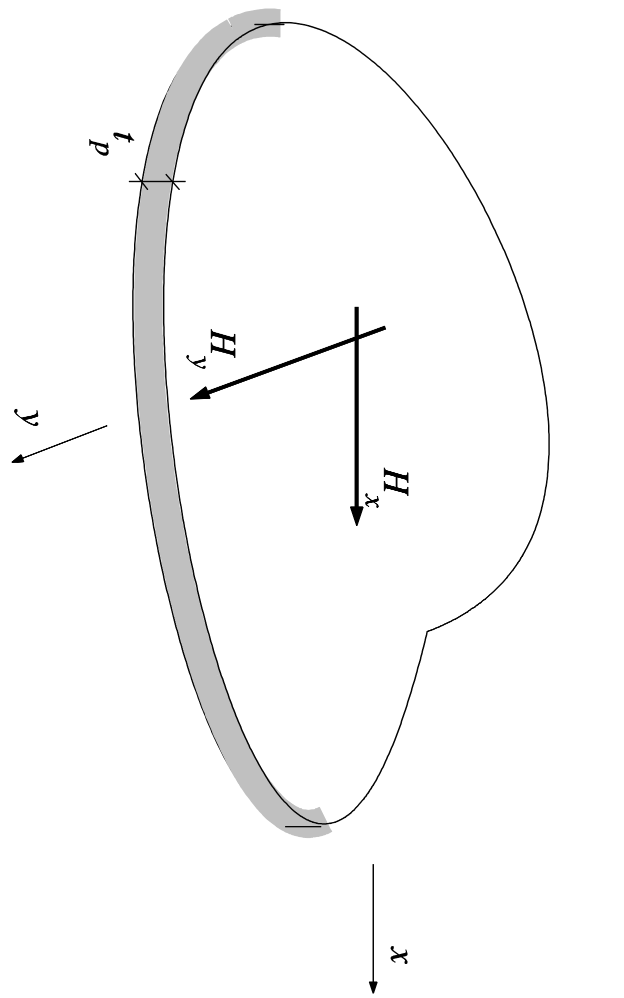

Fig. 1 A continuum-based configuration of an infinite nanoplate immersed in a steady bidirectional in-plane magnetic field

2. Basic assumptions and formulations

2.1 Nonlocal equations of motion

Consider an infinite homogeneous elastic nanoplate of thickness t_p, density ρ_p, Poisson's ratio ν_p, Elasticity modulus E_p as demonstrated in Fig. 1. The nanoplate is acted upon by a steady in-plane biaxially magnetic field represented by: $\mathbf{H}_0 = H_x \hat{e}_x + H_y \hat{e}_y$, where $\mathbf{H}_0$ is the magnetic field vector, and H_x and H_y represent components of the magnetic field along the x and y directions, respectively (see Fig. 1). According to the Kirchhoff plate theory, the displacement field vector of the nanoplate is stated by: $\mathbf{u} = u_x \hat{e}_x + u_y \hat{e}_y + u_z \hat{e}_z$ where $u_x(x,y,z,t) = u_0(x,y,t) - z\, w_{0,x}(x,y,t)$, $u_y(x,y,z,t) = v_0(x,y,t) - z\, w_{0,y}(x,y,t$, and $u_z(x,y,z,t) = w_0(x,y,t)$. In these relations, u_x, u_y, and u_z in order are the displacement components pertinent to the x, y, and z axes, and u_0, v_0 and w_0 are their mid-plane displacements, respectively. For a conducting structure immersed in a steady magnetic field, using Maxwell's electro-magnetic equations, the so-called Lorentz force of the nanoplate could be evaluated from

(Wang, Dong *et al*. 2010, Kiani 2014c)

$$\mathbf{f}_m = \eta\left(\nabla \times \left(\nabla \times (\mathbf{u} \times \mathbf{H}_0)\right)\right) \times \mathbf{H}_0, \tag{1}$$

where η is the magnetic permeability of the nanoplate, $\mathbf{u}$ is the displacement field vector. The generated forces and bending moments within the nanoplate due to the biaxially applied magnetic field are evaluated by: $\mathbf{F}_m = \int_{-t_p/2}^{t_p/2} \mathbf{f}_m dz$ and $\mathbf{M}_m = \int_{-t_p/2}^{t_p/2} z\,\mathbf{f}_m dz$.

By virtue of these relations through using Hamilton's principle, the nonlocal equations of motion of the conducting nanoplate subjected to a biaxially in-plane magnetic field are obtained as

$$N^{nl}_{xx,x} + N^{nl}_{xy,y} = I_0\, u_{0,tt} - \eta t_p H_y^2\left(u_{0,xx} + u_{0,yy}\right), \tag{2a}$$

$$N^{nl}_{xy,x} + N^{nl}_{yy,y} = I_0\, v_{0,tt} - \eta t_p H_x^2\left(v_{0,xx} + v_{0,yy}\right), \tag{2b}$$

$$\begin{aligned} M^{nl}_{xx,xx} + 2M^{nl}_{xy,xy} + M^{nl}_{yy,yy} &= I_0 w_{0,tt} \\ &-I_2\left(w_{0,xxtt} + w_{0,yytt}\right) + \frac{\eta t_p^3}{12} \\ \Big(H_y^2\left(w_{0,xxxx} + w_{0,xxyy}\right) &+ H_x^2\left(w_{0,yyyy} + w_{0,xxyy}\right)\Big) \\ &-\eta t_p\left(H_x^2 - H_y^2\right)\left(w_{0,xx} - w_{0,yy}\right), \end{aligned} \tag{2c}$$

where $I_n = \int_{-t_p/2}^{t_p/2} \rho_p z^n dz$, N^{nl}_{xx} and N^{nl}_{yy} are the nonlocal axial force in the x and y directions, N^{nl}_{xy} is the nonlocal in-plane shear force, M^{nl}_{xx} and M^{nl}_{yy} in order are the nonlocal bending moment about the x and y axes, and M^{nl}_{xy} is the nonlocal twisting moment. All of these nonlocal forces and moments are evaluated per unit length. Eqs. (2a) and (2b) denote the in-plane motions of the conducting nanoplate, whereas, Eq. (2c) describes the out-of-plane vibration of the nanoplate. The nonlocal forces in Eqs. (2a)-(2c) are related to the local ones as follows (Pradhan and Phadikar 2009, Arash, Wang *et al*. 2012, Arash and Wang 2012)

$$N^{nl}_{xx} - (e_0 a)^2\nabla^2 N^{nl}_{xx} = N^l_{xx} = C\left(u_{0,x} + \nu_p v_{0,y}\right), \tag{3a}$$

$$N^{nl}_{yy} - (e_0 a)^2\nabla^2 N^{nl}_{yy} = N^l_{yy} = C\left(v_{0,y} + \nu_p u_{0,x}\right), \tag{3b}$$

$$\begin{aligned} N^{nl}_{xy} - (e_0 a)^2\nabla^2 N^{nl}_{xy} &= N^l_{xy} \\ &= \frac{C}{2}\left(1 - \nu_p\right)\left(u_{0,y} + v_{0,x}\right), \end{aligned} \tag{3c}$$

$$\begin{aligned} M^{nl}_{xx} - (e_0 a)^2\nabla^2 M^{nl}_{xx} &= M^l_{xx} \\ &= -D\left(w_{0,xx} + \nu_p w_{0,yy}\right), \end{aligned} \tag{3d}$$

$$\begin{aligned} M^{nl}_{yy} - (e_0 a)^2\nabla^2 M^{nl}_{yy} &= M^l_{yy} \\ &= -D\left(w_{0,yy} + \nu_p w_{0,xx}\right), \end{aligned} \tag{3e}$$

$$M^{nl}_{xy} - (e_0 a)^2\nabla^2 M^{nl}_{xy} = M^l_{xy} = -D\left(1 - \nu_p\right) w_{0,xy}. \tag{3f}$$

where $e_0 a$ denotes the small-scale parameter, C and D in order are the in-plane and bending rigidity which are expressed by $C=E_p t_p/(1-\nu_p^3)$ and $D=E_p\, t_p^3/(12(1-\nu_p^3))$. The small-scale parameter is commonly determined by comparing the predicted dispersions curves by the nonlocal model with those of another atmoistic-based methodology. By combining Eqs. (2a)-(2c) and Eqs. (3a)-(3f), through using the following dimensionless quantities and operators

$$\begin{aligned} &\overline{u}_0 = \frac{u_0}{t_p}, \overline{v}_0 = \frac{v_0}{t_p}, \overline{w}_0 = \frac{w_0}{t_p}, \xi = \frac{x}{t_p}, \eta = \frac{y}{t_p}, \\ &t = t_p^2\sqrt{\frac{I_0}{D}}\tau, \mu = \frac{e_0 a}{t_p}, \overline{C} = \frac{C t_p^2}{D}, \overline{I}_2 = \frac{I_2}{I_0 t_p^2}, \\ &\Xi[.] = [.] - \mu^2\left([.]_{,\xi\xi} + [.]_{,\eta\eta}\right), \\ &\overline{H}_x = H_x\sqrt{\frac{\eta t_p^3}{D}}, \overline{H}_y = H_y\sqrt{\frac{\eta t_p^3}{D}}, \\ &\overline{\nabla}^2[.] = [.]_{,\xi\xi} + [.]_{,\eta\eta}, \overline{\nabla}^4[.] \\ &= [.]_{,\xi\xi\xi\xi} + 2[.]_{,\xi\xi\eta\eta} + [.]_{,\eta\eta\eta\eta}, \end{aligned} \tag{4}$$

the dimensionless nonlocal governing equations of the problem under study are derived

$$\begin{aligned} &\overline{C}\left(\overline{u}_{0,\xi\xi} + \frac{1-\nu_p}{2}\overline{u}_{0,\eta\eta} + \frac{1+\nu_p}{2}\overline{v}_{0,\xi\eta}\right) \\ &\quad + \overline{H}_y^2\Xi\{\overline{u}_{0,\xi\xi} + \overline{u}_{0,\eta\eta}\} = \Xi\{\overline{u}_{0,\tau\tau}\} \end{aligned} \tag{5a}$$

$$\begin{aligned} &\overline{C}\left(\overline{v}_{0,\eta\eta} + \frac{1-\nu_p}{2}\overline{v}_{0,\xi\xi} + \frac{1+\nu_p}{2}\overline{u}_{0,\xi\eta}\right) \\ &\quad + \overline{H}_x^2\Xi\{\overline{v}_{0,\xi\xi} + \overline{v}_{0,\eta\eta}\} = \Xi\{\overline{v}_{0,\tau\tau}\} \end{aligned} \tag{5b}$$

$$\begin{aligned} &\overline{\nabla}^4\overline{w}_0 + \frac{1}{12}\Xi\left\{\overline{H}_y^2\overline{\nabla}^2\overline{w}_{0,\xi\xi} + \overline{H}_x^2\overline{\nabla}^2\overline{w}_{0,\eta\eta}\right\} - \\ &\left(\overline{H}_x^2 - \overline{H}_y^2\right)\Xi\{\overline{w}_{0,\xi\xi} - \overline{w}_{0,\eta\eta}\} = \\ &\Xi\{\overline{w}_{0,\tau\tau} - \overline{I}_2\left(\overline{w}_{0,\tau\tau\xi\xi} + \overline{w}_{0,\tau\tau\eta\eta}\right)\} \end{aligned} \tag{5c}$$

where τ and μ represent the dimensionless time and small-scale parameters, respectively.

2.2 Arbitrarily propagated in-plane and out-of-plane waves

Let harmonic elastic waves propagate within the nanoplate along the $\mathbf{r}$ direction of angle ϕ with respect to the x axis as in the following form

$$< u_0, v_0, w_0 > = < U_0, V_0, W_0 > e^{\mathrm{i}(\mathbf{k}.\mathbf{r} - \omega t)}, \tag{6}$$

where U_0, V_0, and W_0 are the amplitudes of the waves along the x, y, and z axes, respectively, $i = \sqrt{-1}$, $\mathbf{k} = k_x\hat{e}_x + k_y\hat{e}_y$ is the wave vector, $k_x = k\cos\phi$ and $k_y = k\sin\phi$, k is the wavenumber, $\mathbf{r} = r\hat{e}_r = x\hat{e}_x + y\hat{e}_y$ denotes the position vector, $\hat{e}_x$, $\hat{e}_y$, and $\hat{e}_r$ in order are the unit vectors pertinent to the x, y, and $\mathbf{r}$ directions, and ω is the wave's frequency. According to Eq. (4), Eq. (6) could be rewritten in the following dimensionless form as well

$$< \overline{u}_0, \overline{v}_0, \overline{w}_0 > = < \overline{U}_0, \overline{V}_0, \overline{W}_0 > e^{\mathrm{i}(\overline{\mathbf{k}}.\overline{\mathbf{r}} - \varpi\tau)}, \tag{7}$$

where the dimensionless quantities in Eq. (7) are as

$$\overline{U}_0 = \frac{U_0}{t_p}, \overline{V}_0 = \frac{V_0}{t_p}, \overline{W}_0 = \frac{W_0}{t_p}, \overline{\mathbf{k}} = \overline{k}_x\hat{e}_x + \overline{k}_y\hat{e}_y, \overline{k}_x = t_p\, k_x, \tag{8}$$

$$\overline{k}_y = t_p\, k_y, \overline{k} = \sqrt{\overline{k}_x^2 + \overline{k}_y^2}, \overline{\mathbf{r}} = \xi \hat{e}_x + \eta \hat{e}_y, \varpi = \omega t_p^2 \sqrt{\frac{I_0}{D}}.$$

2.2.1 In-plane and out-of-plane frequencies

By substituting Eq. (7) into Eqs. (5a)-(5c), one can arrive at the following set of algebraic equations

$$\left(-\varpi^2 \begin{bmatrix} 1 & 0 & 0 \\ 0 & 1 & 0 \\ 0 & 0 & 1 \end{bmatrix} + \begin{bmatrix} \Gamma_1 & \Gamma_2 & 0 \\ \Gamma_2 & \Gamma_3 & 0 \\ 0 & 0 & \Gamma_4 \end{bmatrix}\right) \begin{Bmatrix} \overline{U}_0 \\ \overline{V}_0 \\ \overline{W}_0 \end{Bmatrix} = \begin{Bmatrix} 0 \\ 0 \\ 0 \end{Bmatrix}, \tag{9}$$

where

$$\Gamma_1 = \frac{\overline{C}\,\overline{k}^2}{1+\mu^2\overline{k}^2}\left((\cos\phi)^2 + \frac{1-\nu_p}{2}(\sin\phi)^2\right) + \left(\overline{k}\,\overline{H}_y\right)^2, \tag{10a}$$

$$\Gamma_2 = \frac{(1+\nu_p)\overline{C}\,\overline{k}^2}{4\left(1+\mu^2\overline{k}^2\right)}\sin(2\phi), \tag{10b}$$

$$\Gamma_3 = \frac{\overline{C}\,\overline{k}^2}{1+\mu^2\overline{k}^2}\left(\frac{1-\nu_p}{2}(\cos\phi)^2 + (\sin\phi)^2\right) + \left(\overline{k}\,\overline{H}_x\right)^2, \tag{10c}$$

$$\Gamma_4 = \frac{\overline{k}^4}{1+\mu^2\overline{k}^2} + \frac{1}{1+\overline{I}_2\overline{k}^2} \left\{\frac{\overline{k}^4}{12}\left[\left(\overline{H}_x\sin\phi\right)^2 + \left(\overline{H}_y\cos\phi\right)^2\right] + \overline{k}^2\left[\left(\overline{H}_x^2 - \overline{H}_y^2\right)\cos(2\phi) + 2\overline{H}_x\overline{H}_y\sin(2\phi)\right]\right\}. \tag{10d}$$

By setting the determinant of the coefficient matrix in Eq. (9) equal to zero, a nontrivial solution to the set of equations could be obtained. As a result

$$\varpi_{in_1} = \sqrt{\frac{\Gamma_1 + \Gamma_3 - \sqrt{(\Gamma_1-\Gamma_3)^2 + 4\Gamma_2^2}}{2}}, \tag{11a}$$

$$\varpi_{in_2} = \sqrt{\frac{\Gamma_1 + \Gamma_3 + \sqrt{(\Gamma_1-\Gamma_3)^2 + 4\Gamma_2^2}}{2}}, \tag{11b}$$

$$\varpi_{out} = \sqrt{\Gamma_4}, \tag{11c}$$

where ϖ_{in_1} and ϖ_{in_2} are the dimensionless frequencies pertinent to the in-plane waves, called in-plane frequencies, and ϖ_{out} is the dimensionless frequency associated with the out-of-plane motion of the conducting nanoplate exposed to biaxially in-plane magnetic field. The latter one is also called flexural, transverse, or out-of-plane frequency.

2.2.2 In-plane and out-of-plane phase velocities

The phase velocity vector, $\mathbf{C}_p$, is defined as

$$\mathbf{C}_p = C_p\hat{e}_r; C_p = \frac{\omega}{k} = \frac{\varpi}{t_p\overline{k}}\sqrt{\frac{D}{I_0}}, \tag{12}$$

where C_p is the phase velocity (magnitude) pertinent to the frequency ω. By introducing Eqs. (11a)-(11c) to Eq. (12), the phase velocities of the in-plane and out-of-plane waves are obtained.

2.2.3 In-plane and out-of-plane group velocities

The group velocity vector of the propagated waves within the nanoplate is given by

$$\mathbf{C}_g = \frac{\partial\omega}{\partial k}\,\hat{e}_r + \frac{1}{k}\frac{\partial\omega}{\partial\phi}\hat{e}_\phi = \frac{1}{t_p}\sqrt{\frac{D}{I_0}}\left(\frac{\partial\varpi}{\partial\overline{k}}\,\hat{e}_r + \frac{1}{\overline{k}}\frac{\partial\varpi}{\partial\phi}\,\hat{e}_\phi\right), \tag{13}$$

and the magnitude of the group velocity is determined by

$$C_g = \frac{1}{t_p}\sqrt{\frac{D}{I_0}}\sqrt{\left(\frac{\partial\varpi}{\partial\overline{k}}\right)^2 + \left(\frac{1}{\overline{k}}\frac{\partial\varpi}{\partial\phi}\right)^2}, \tag{14}$$

in which the first derivative of ϖ with respect to ϕ and $\overline{k}$ could be readily calculated by using Eqs. (11a)-(11c) and Eqs. (10a)-(10d).

3. Results and discussion

To investigate the characteristics of the propagated in-plane and out-of-plane waves within conducting nanoplates subjected to biaxially in-plane magnetic field, a fairly comprehensive parametric study is performed. To this end, a nanoplate is considered with the following geometry and mechanical data: $t_p = 2$ nm, $e_0a = 2$ nm, $\rho_p = 2300$ kg/m ^{3}, $E_p = 1$ TPa, and $\nu_p = 0.25$. In the following, the effects of wavenumber and direction of the propagated waves as well as strength of the applied magnetic fields on the in-plane and out-of-plane frequencies as well as phase and group velocities are studied.

The cut-off frequencies pertinent to both in-plane and out-of-plane waves have not been discussed. These frequencies are evaluated from the general formulations of in-plane and out-of-plane frequencies, namely Eqs. (11a)-(11c), as the wavenumber approaches zero. It could be readily proved that all cut-off frequencies are equal to zero since the nanoplate has not been constrained elastically against in-plane and out-of-plane motions.

3.1 Several verifications

In the first comparison study, the predicted out-of-plane frequencies of the magnetically affected nanoplate are checked with those of suggested model by Narendar and Gopalakrishnan (2012) in a special case. They studied characteristics of flexural waves in thin nanoplates under thermal effect using nonlocal Kirchhoff plate theory. In the absence of the magnetic field (i.e., $H_x = H_y = 0$), the dimensionless flexural frequency is calculated using Eq. (11c):

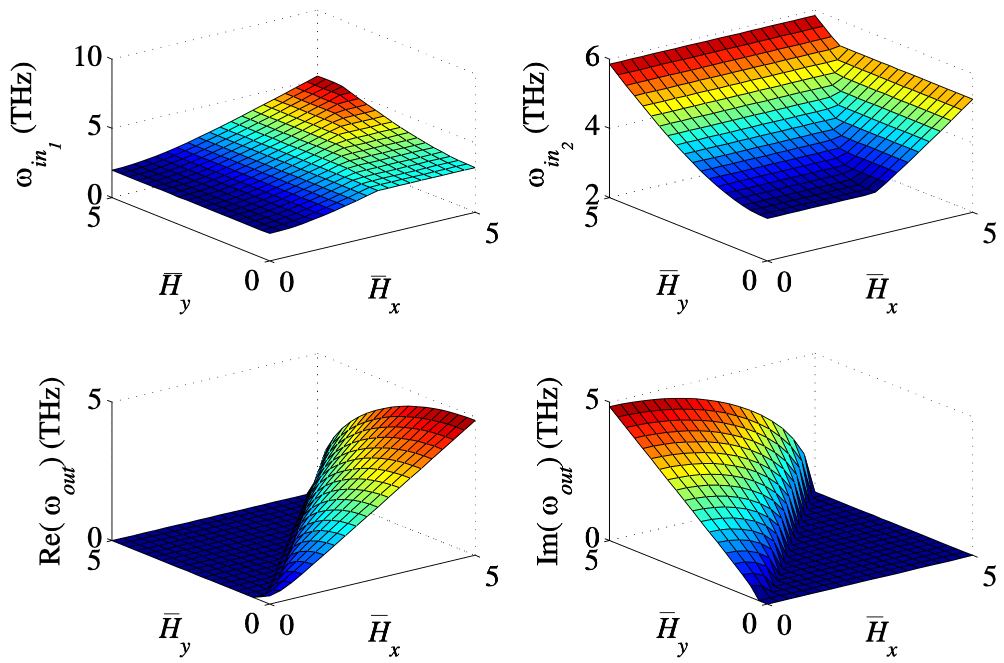

Fig. 2 The frequencies of the waves propagate within the conducting nanoplate along the x axis (i.e., $\phi = 0$) in terms of the strength of the biaxially magnetic field ($\overline{k} = \frac{\pi}{10}$)

$\varpi_{out} = \overline{k}^2/\sqrt{1+(\mu\overline{k})^2}$. It can be also stated in terms of dimensional parameters of the nanoplate, wavenumbers, and small-scale parameter as follows

$$\omega_{out} = \sqrt{\frac{D}{I_0}}\,\frac{k_x^2+k_y^2}{\sqrt{1+(e_0a)^2\left(k_x^2+k_y^2\right)}}. \qquad (15)$$

In the case of only wave propagation along the y direction (i.e., k_x=0), the given expression in Eq. (15) is identical to that predicted by the model of Narendar and Gopalakrishnan (2012) when the thermal effect is neglected.

In another verification study, we check the obtained in-plane frequencies with those of Wang, Dong *et al.* (2010) for a particular case. Using a nonlocal elasticity model, they investigated characteristics of longitudinal waves in elastic nanoplates. Herein, the strength of in-plane magnetic field is set equal to zero. In view of Eqs. (11a) and (11b), the frequencies of the general in-plane waves are expressed by

$$\omega_{in_1} = \sqrt{\frac{E_p}{2(1+\nu_p)}}\,\frac{\sqrt{k_x^2+k_y^2}}{\sqrt{1+(e_0a)^2(k_x^2+k_y^2)}}, \qquad (16a)$$

$$\omega_{in_2} = \sqrt{\frac{E_p}{1-\nu_p^2}}\,\frac{\sqrt{k_x^2+k_y^2}}{\sqrt{1+(e_0a)^2(k_x^2+k_y^2)}}. \qquad (16b)$$

In a special case that the in-plane waves propagate along the x direction (i.e., k_y=0), the in-plane displacements are not coupled. In such a case, the largest frequency resulted from Eqs. (16a) and (16b) represents the frequency of the longitudinal wave and it is provided by

$$\omega_{in} = \sqrt{\frac{E_p}{1-\nu_p^2}}\,\frac{k_x}{\sqrt{1+(e_0a)^2\,k_x^2}}. \qquad (17)$$

The obtained frequency in Eq. (17) is the same as that predicted by the model of Wang *et al.* (2010).

3.2 Effect of the magnetic field strength on the frequencies of in-plane and out-of-plane waves

In Fig. 2, the frequencies of the in-plane and out-of-plane propagated waves within the conducting nanoplate are demonstrated as a function of the strength of biaxially magnetic field. These plots are provided for the case of $\phi = 0$ and $\overline{k} = \frac{\pi}{10}$. As it is seen, both in-plane frequencies magnify with the strength of the in-plane magnetic field in each direction. For $\overline{H}_x < 2.5$, the variation of the magnetic field strength in the y (x) direction has a trivial effect on the variation of the lower (higher) in-plane frequency. However, for $\overline{H}_x > 2.5$, the variation of $\overline{H}_y$ ($\overline{H}_x$) is more influential on the variation of the lower (higher) in-plane frequency. According to the plotted results in Fig. 2, the flexural frequency increases with the strength of the magnetic field along the direction of wave propagation, however, the application of the perpendicular magnetic field would result in a decrease in the flexural frequency. As it is observed, for $H_y \approx H_x$, the flexural frequency vanishes, and for $H_y > H_x$, the real part of the flexural frequency becomes zero whereas the imaginary part is positive. In such a condition, the flexural wave would not be propagated through the conducting nanoplate since its amplitudes would decay with the time. Such a fact guides

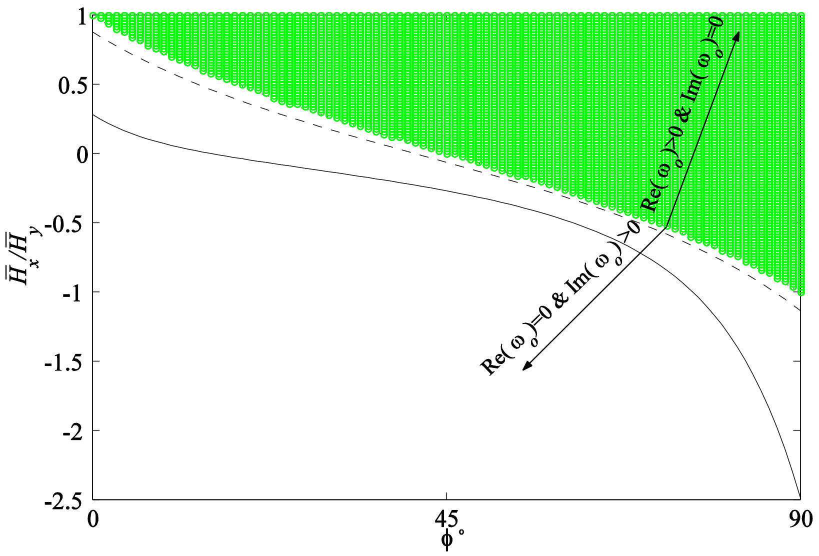

Fig. 3 Transmissibility zones of the plane $\frac{\bar{H}_x}{\bar{H}_y}$-$\phi$ for three levels of the wavenumber of the transverse waves; (The colorful area and that without color show the regions where the propagation of the flexural waves would be possible and impossible, respectively. The interfaces of each two specified zones are demonstrated by dotted, dashed, and solid lines for the cases $\bar{k}=\frac{\pi}{10},\frac{\pi}{2}$, and π, respectively; $\bar{H}_y=10$)

us to determine the conditions in which the magnetically exposed nanoplate would not be a suitable nano-device for appropriate transmission of the flexural waves.

3.3 The conditions that the waves could not be transmitted

In this part, we are interested in finding circumferences where the sound waves would not be appropriately propagated within the magnetically exposed nanoplate. Regarding the in-plane waves, a close scrutiny reveals that the expressions under the radical in Eqs. (11a) and (11b) are always positive. Thereby, the in-plane waves are expected to be transmitted through the nanoplate for all levels of the wavenumber and the strength of the in-plane magnetic field. Moreover, their frequencies could be efficiently controlled by application of appropriate in-plane magnetic field as discussed in the previous part. Concerning the out-of-plane waves, a detailed investigation shows that their frequencies would become zero under special circumferences. Such a scrutiny guides us to the condition guarantees propagation of the flexural waves, namely $\Gamma_4>0$. Hence

$$\left(\frac{\bar{H}_x}{\bar{H}_y}\right)^2\left(\frac{\bar{k}^2}{12}(\sin\phi)^2+\cos(2\phi)\right)+2\left(\frac{\bar{H}_x}{\bar{H}_y}\right)\sin(2\phi)+ \left(\frac{\bar{k}^2}{12}(cos\phi)^2-\cos(2\phi)+\frac{\bar{k}^2}{\left(1+\bar{I}_2\bar{k}^2\right)\bar{H}_y^2}\right)>0, \tag{18}$$

Eq. (18) explains that the magnitudes of the components of the in-plane magnetic field, thickness of the nanoplate, wavenumber, and the direction of the wave are among the influential factors control propagation of the flexural waves within the conducting nanoplate. In Fig. 3, the areas with color and without color, respectively, denote the zones that the propagation of flexural waves would be possible and impossible. For the conducting nanoplate under study, the interfaces of such zones could be clearly specified via Eq. (18). In the case of $\bar{H}_y=10$, the interfaces presented by the dotted, dashed, and solid lines in order are pertinent to $\bar{k}=\frac{\pi}{10},\frac{\pi}{2}, and \pi$. As it is observed in Fig. 3, the range of the magnetic field along the x direction which is of interest for propagating the flexural waves generally magnifies with the angle of the wave direction with respect to the x axis as well as the wavenumber.

3.4 Effect of the wavenumber on characteristics of in-plane and out-of-plane waves

In Fig. 4, the in-plane and out-of-plane frequencies as well as their corresponding phase and group velocities as a function of dimensionless wavenumber are provided for different levels of the strength of the in-plane magnetic field. The results are plotted in the case of propagation of the wave along the diagonal of the square nanoplate. In the absence of the magnetic field, both in-plane frequencies converge to specific values as the wavenumber increases. However, in the presence of the in-plane magnetic field, due to the appearance of terms $(\bar{k}\,\bar{H}_x)^2$ and $(\bar{k}\,\bar{H}_y)^2$ in the expressions of Γ_1 and Γ_3 , the in-plane frequencies commonly magnify with the wavenumber. The flexural frequency commonly magnifies with the wavenumber. The variation rate of the flexural frequency in terms of the wavenumber is more obvious for higher levels of the strength of in-plane magnetic field. Generally, for lower levels of the in-plane magnetic field, the rate of variation of the phase velocities as a function of the wavenumber is more apparent. In other words, for higher levels of the applied magnetic field in both directions, variation of the

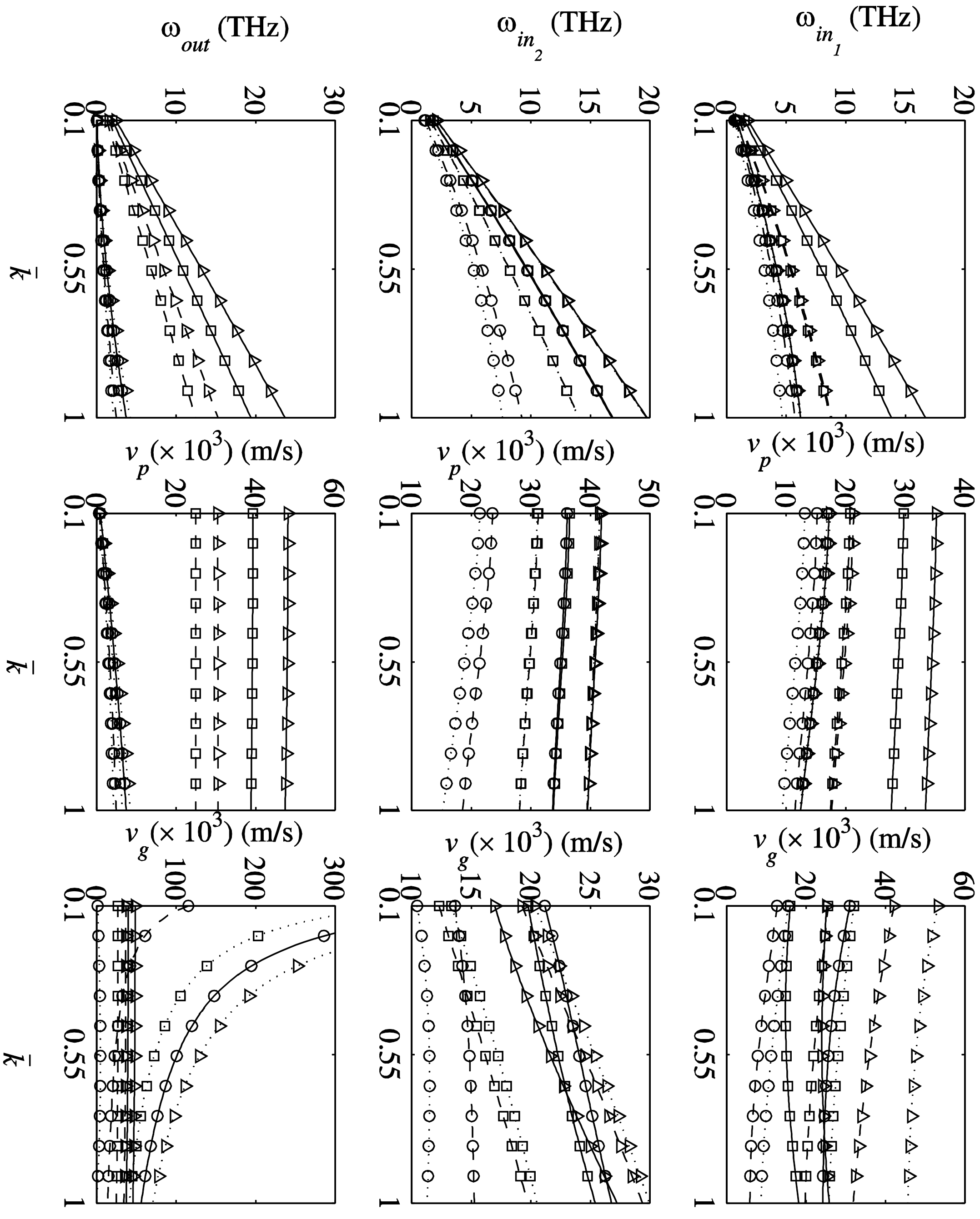

Fig. 4 Plots of frequencies, phase velocities, and group velocities of the in-plane and out-of-plane waves propagate along the diagonal of the conducting nanoplate (i.e., $\phi = \frac{\pi}{4}$) in terms of the wavenumber for various levels of the magnetic field strength: ((...) $\overline{H}_x = 0$, $(- - -)$ $\overline{H}_x = 2$, (—) $\overline{H}_x = 5$; (∘) $\overline{H}_y = 0$, (□) $\overline{H}_y = 4$, (Δ) $\overline{H}_y = 6$)

wavenumber has a lower influence on the variation of both in-plane and out-of-plane phase velocities.

3.5 Effect of the wave direction on its characteristics

Herein, we are interested in the role of the wave direction on the characteristics of the in-plane and out-of-plane waves. In the case of $\overline{k} = \pi$, the plots of the frequencies as well as their corresponding phase and group velocities as a function of the angle of wave direction are provided in Fig. 5. In the absence of the in-plane magnetic field, the characteristics of both in-plane and out-of-plane waves are independent from the wave direction. According to the plotted results in Fig. 5, in the presence of the in-plane magnetic field, the characteristics of the in-plane waves would not rely on ϕ if and only if identical magnetic fields are applied in both x and y directions (i.e., $H_x = H_y$). Further, the predicted in-plane frequencies as well as their corresponding phase velocities of the symmetrically propagated waves with respect to the x axis are symmetric. However, this fact is not commonly true for the out-of-plane waves, except in the case of $H_y = 0$.

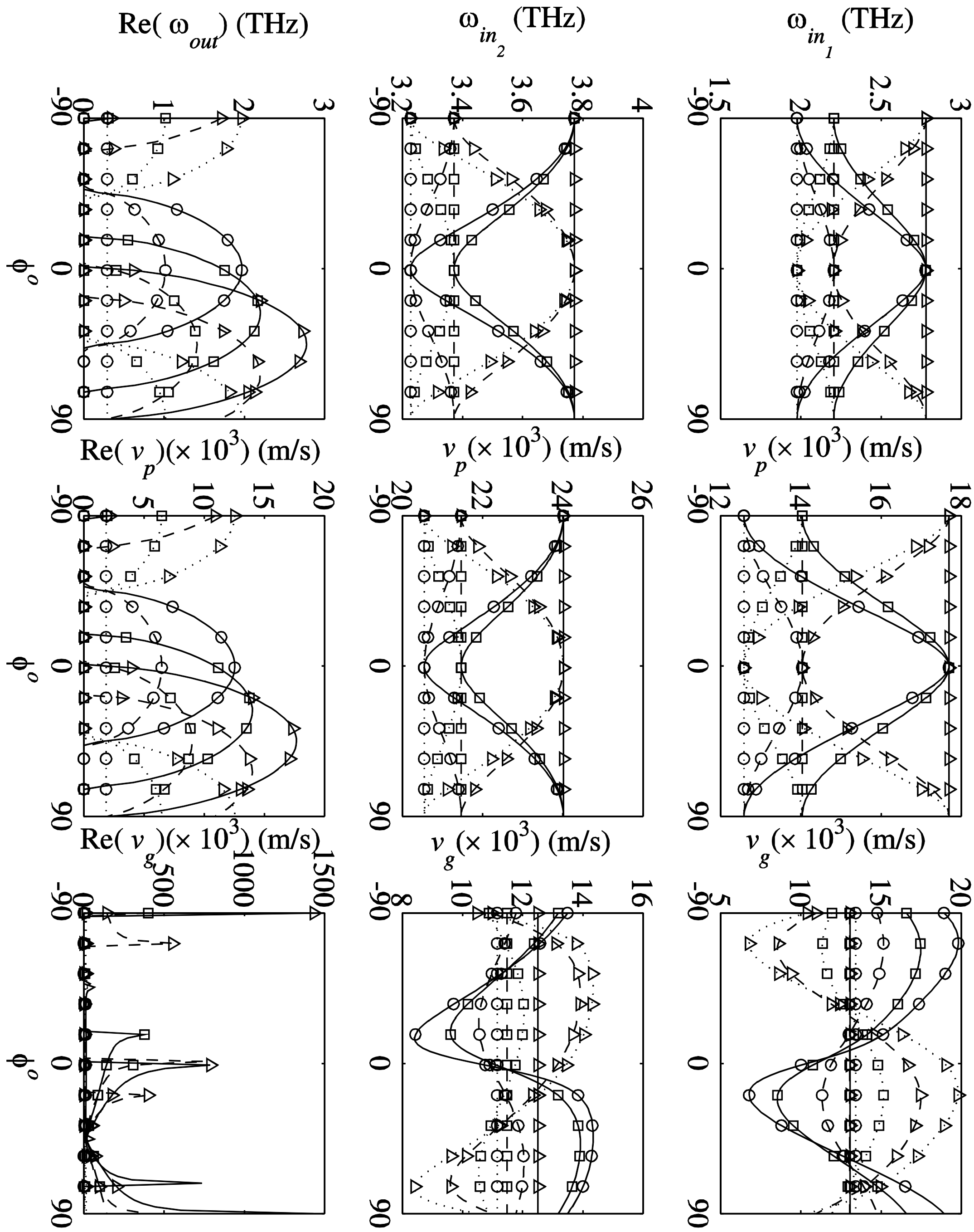

Fig. 5 Plots of frequencies, phase velocities, and group velocities of the in-plane and out-of-plane waves with $\overline{k} = \frac{\pi}{10}$ in terms of the angle of direction of waves for various levels of the magnetic field strength: ((…) $\overline{H}_x = 0$, (− − −) $\overline{H}_x = 1$, (—) $\overline{H}_x = 2$; (∘) $\overline{H}_y = 0$, (□) $\overline{H}_y = 1$, (Δ) $\overline{H}_y = 2$)

3.6 Effect of the small-scale parameter on characteristics of in-plane and out-of-plane waves

Fig. 6 shows variation of the in-plane frequencies and flexural frequency as a function of the small-scale parameter for various levels of the components of magnetic field. The considered wave propagates along the x axis with $\overline{k} = \pi$. Concerning in-plane waves, their corresponding frequencies, phase velocities, and group velocities would reduce by an increase of the small-scale parameter. In fact, the predicted characteristics of the in-plane waves based on the NCT are overestimated by the CCT. Additionally, the influence of the small-scale parameter on the second in-plane frequencies is more obvious. A close survey of the obtained results reveals that the role of the small-scale parameter on the characteristics of the in-plane waves propagated in the x direction are enhanced by increasing of the components of the magnetic field. Regarding the out-of-plane waves, both flexural frequency and phase velocity would lessen as the effect of the small-scale parameter becomes more pronounce.

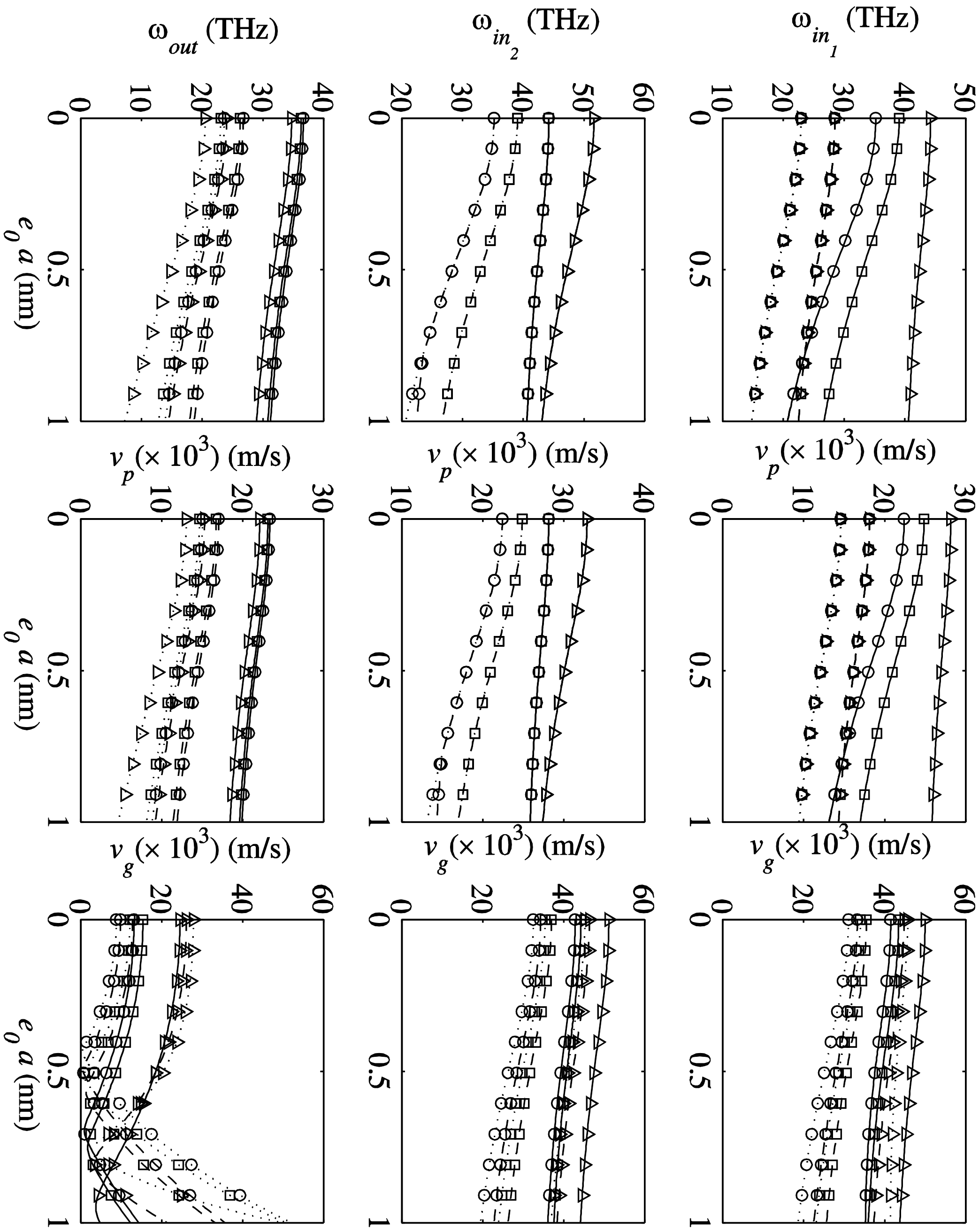

Fig. 6 Plots of frequencies, phase velocities, and group velocities of the in-plane and out-of-plane waves propagate along the x axis of the conducting nanoplate (i.e., $\phi = 0$) in terms of the small-scale parameter for various levels of the magnetic field strength: ((…) $\overline{H}_x = 1$, ($- - -$) $\overline{H}_x = 2$, (—) $\overline{H}_x = 4$; (∘) $\overline{H}_y = 1$, (□) $\overline{H}_y = 2$, (Δ) $\overline{H}_y = 4$)

However, the group velocity of such waves would generally reduce with the small-scale parameter up to a particular value of the small-scale parameter. For small-scale parameters greater than these values, the group velocity would increase by an increase of the small-scale parameter. By increasing the strength of the magnetic field along the y direction, both flexural frequency and its phase velocity would decrease; however, these values would grow by an increase of the x component of the magnetic field. As it is seen, the CCT overestimates the flexural frequency and its corresponding phase velocity based on the NCT. As the strength of the magnetic field along the y direction increases and that of the x direction lessens, the influence of the small-scale parameter on the out-of-plane frequencies and their corresponding phase velocities becomes more apparent. In such conditions, the discrepancies between the predicted results by the NCT and those of the CCT are more obvious.

3.7 Effect of the thickness on characteristics of the in-plane and out-of-plane waves

The most important geometrical feature of the nanoplate is its thickness. Herein we are interested in exploring the

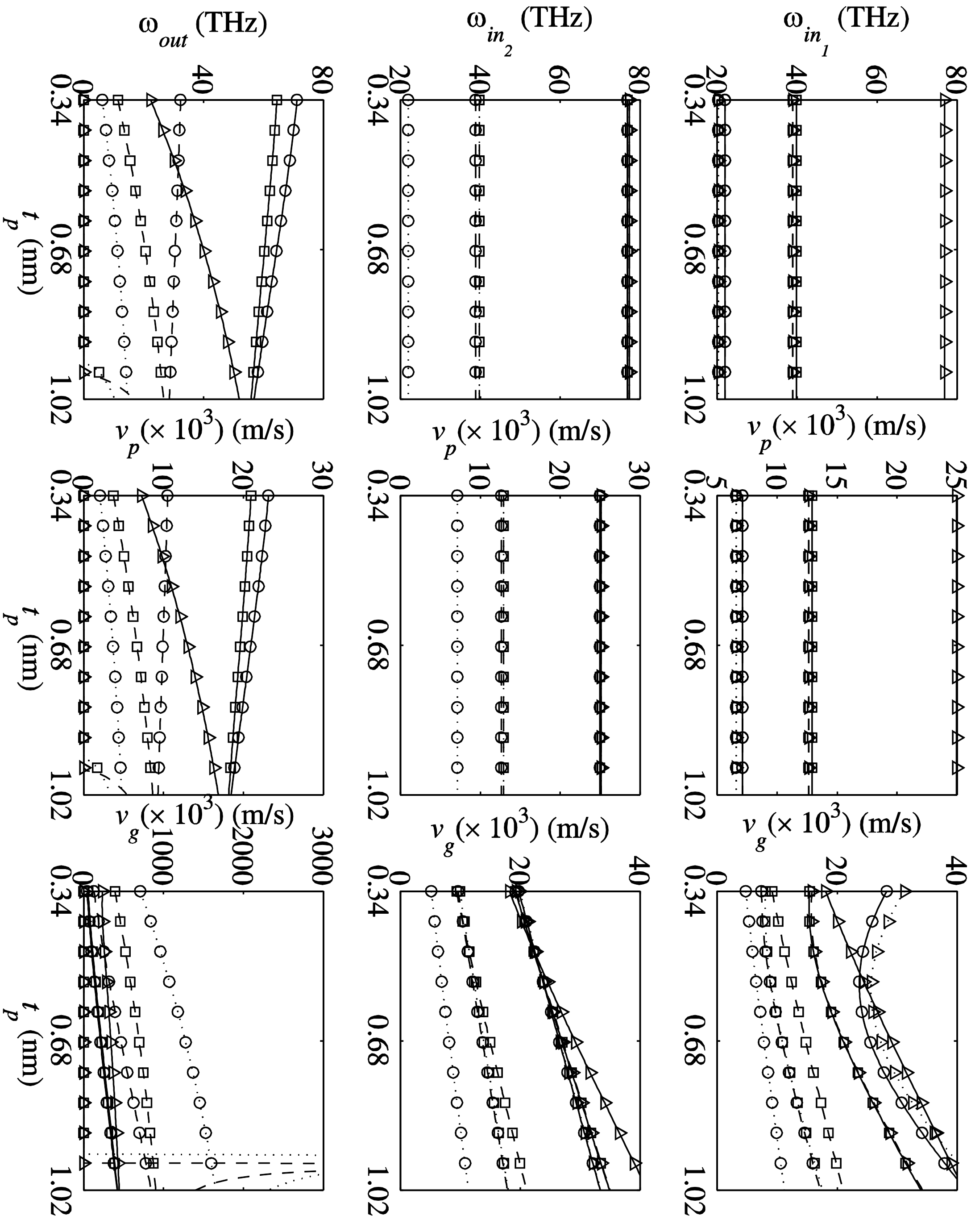

Fig. 7 Plots of frequencies, phase velocities, and group velocities of the in-plane and out-of-plane waves propagate along the x axis of the conducting nanoplate (i.e., $\phi = 0$) in terms of the nanoplate's thickness for various levels of the magnetic field strength: $((\ldots)\ \overline{H}_x = 1$, $(- - -)\ \overline{H}_x = 2$, $(—)\ \overline{H}_x = 4$; $(\circ)\ \overline{H}_y = 1$, $(\square)\ \overline{H}_y = 2$, $(\Delta)\ \overline{H}_y = 4)$

role of the nanoplate's thickness on the characteristics of both in-plane and out-of-plane waves. In Fig. 7, the plots of the frequencies and their corresponding phase and group velocities as a function of thickness have been plotted for different levels of strength of the magnetic field along the x and y axis. The plotted results are provided in the case of ϕ=0, and $\overline{k} = \overline{k}_0\, t_p/t_{p0}$ where t_{p0}=1.02 nm and $\overline{k}_0$=π. According to the obtained results, variation of the thickness has no influence on the variations of the in-plane frequencies and their corresponding phase velocities. However, these factors are affected by the strength of the magnetic field in both directions. In fact, the in-plane frequencies would magnify as the strength of the magnetic field in both directions grows. It implies that the strength of the magnetic field is the dominant factor in controlling the in-plane vibration of conducting nanoplates. Additionally, the group velocity of in-plane waves would generally magnify by increasing of the nanoplate's thickness. Concerning the out-of-plane vibration of the conducting nanoplate, the trends of the characteristics of the out-of-plane waves highly rely on the strength of the applied magnetic field. For example, in the case of $\overline{H}_x=\overline{H}_y=4$, flexural frequencies as well as phase and group velocities would grow by an increase of the nanoplate's thickness; nevertheless, in the cases of $\overline{H}_x$=4 and $\overline{H}_y$=1 and 2, flexural frequency and phase velocity would reduce by increasing of the nanoplate's thickness. Further, in the cases of ($\overline{H}_x$,$\overline{H}_y$)=(1,2), (1,4), and (2,4), the real part of the flexural frequency becomes zero for values of thickness lower than certain values. It indicates that the out-of-plane waves are damped for such a range of the nanoplate's thickness. For values of thickness greater than this particular value, both flexural frequency and phase velocity would grow by an increase of the thickness. Irrespective of the magnitudes of the exerted in-plane magnetic fields, the group velocities of out-of-plane waves would commonly grow as the thickness increases.

4. Conclusions

Using nonlocal continuum theory of Eringen, wave propagation within conducting nanoplates immersed in biaxially in-plane magnetic fields are examined. By employing Maxwell's electro-magnetic equations as well as Lorentz's force, the nonlocal equations of motion of the conducting nanoplate in which describe its in-plane and out-of-plane motions are obtained. Assuming a harmonic form for the propagated waves, the in-plane and out-of-plane frequencies as well as their corresponding phase and group velocities are derived. The influences of the wavenumber, direction of the wave propagation, strength of the in-plane magnetic field, small-scale parameter, and thickness on the above-mentioned characteristics of the waves are explained. The capabilities of the conducting nanoplate in transferring the in-plane and out-of-plane waves are also investigated in some detail. The results reveal that the in-plane frequencies are commonly enhanced by application of the in-plane magnetic field. However, the transmissibility of the out-of-plane wave robustly relies on the strength of the in-plane magnetic field, direction of the propagated transverse wave, small-scale parameter, and thickness of the nanoplate. The criterion for safe propagation of the out-of-plane waves within the conducting nanoplate exposed to a biaxially magnetic field is also extracted.

References

Aifantis, E.C. (1992), "On the role of gradients in the localization of deformation and fracture", *Int. J. Eng. Sci.*, **30**, 1279-1299.

Abouzar, M.H., Poghossian, A., Pedraza, A.M., Gandhi, D., Ingebrandt, S., Moritz, W. and Schoning, M.J. (2011), "An array of field-effect nanoplate SOI capacitors for (bio-)chemical sensing", *Biosens. Bioelectron.*, **26**, 3023-3028.

Aksencer, T. and Aydogdu, M. (2012), "Forced transverse vibration of nanoplates using nonlocal elasticity", *Phys. E*, **44**, 1752-1759.

Ansari, R., Arash, B. and Rouhi, H. (2011), "Vibration characteristics of embedded multi-layered graphene sheets with different boundary conditions via nonlocal elasticity", *Compos. Struct.*, **93**, 2419-2429.

Ansari, R. and Gholami, R. (2016), "Size-dependent nonlinear vibrations of first-order shear deformable magneto-electro-thermo elastic nanoplates based on the nonlocal elasticity theory", *Int. J. Appl. Mech.*, **8**, 1650053.

Ansari, R., Rajabiehfard, R. and Arash, B. (2010), "Nonlocal finite element model for vibrations of embedded multi-layered graphene sheets", *Comput. Mater. Sci.*, **49**, 831-838.

Ansari, R., Sahmani, S. and Arash, B. (2010), "Nonlocal plate model for free vibrations of single-layered graphene sheets", *Phys. Lett. A*, **375**, 53-62.

Ansari, R., Shahabodini, A. and Rouhi, H. (2015), "A nonlocal plate model incorporating interatomic potentials for vibrations of graphene with arbitrary edge conditions", *Curr. Appl. Phys.*, **15**, 1062-1069.

Arash, B. and Wang, Q. (2012), "A review on the application of nonlocal elastic models in modeling of carbon nanotubes and graphenes", *Comp. Mater. Sci.*, **51**, 303-313.

Arash, B., Wang, Q. and Liew, K.M. (2012), "Wave propagation in graphene sheets with nonlocal elastic theory using finite element formulation", *Comput. Meth. Appl. M.*, **223**, 1-9.

Assadi, A. (2013), "Size dependent forced vibration of nanoplates with consideration of surface effects", *Appl. Math. Model.*, **37**, 3575-3588.

Assadi, A. and Farshi, B. (2010), "Vibration characteristics of circular nanoplates", *J. Appl. Phys.*, **108**, 074312.

Chen, J., Lim, B., Lee, E.P. and Xia Y. (2009), "Shape-controlled synthesis of platinum nanocrystals for catalytic and electrocatalytic applications", *Nano Today*, **4**, 81-95.

Clark, D., Wood, D. and Erb, U. (1997), "Industrial applications of electrodeposited nanocrystals", *Nanostruct. Mater.*, **9**, 755-758.

Cosserat, E. and Cosserat, F. (1909), *Theorie des Corps Deformables*, Hermann et Fils, Paris.

Eringen, A.C. (1972), "Linear theory of nonlocal elasticity and dispersion of plane waves", *Int. J. Eng. Sci.*, **10**, 425-435.

Eringen, A.C. (1983), "On differential equations of nonlocal elasticity and solutions of screw dislocation and surface waves", *J. Appl. Phys.*, **54**, 4703-4710.

Eringen, A.C. and Edelen, D.G.B. (1972), "On nonlocal elasticity", *Int. J. Eng. Sci.*, **10**, 233-248.

Fatemi, H., Khodadadi, A.A., Firooz, A.A., Mortazavi, Y. (2012), "Apple-biomorphic synthesis of porous ZnO nanostructures for glucose direct electrochemical biosensor", *Curr. Appl. Phys.*, **2**, 1033-1038.

Grzelczak, M., Perez-Juste, J., Mulvaney, P. and Liz-Marzan, L.M. (2008), "Shape control in gold nanoparticle synthesis", *Chem. Soc. Rev.*, **37**, 1783-1791.

Huang, H., Chen, H., Sun, D. and Wang, X. (2012), "Graphene nanoplate-Pt composite as a high performance electrocatalyst for direct methanol fuel cells", *J. Power Sour.*, **204**, 46-52.

Huang, H. and Wang, X. (2011), "Graphene nanoplate-MnO_2 composites for supercapacitors: a controllable oxidation approach", *Nanoscale*, **3**, 3185-3191.

Jomehzadeh, E. and Saidi, A.R. (2011), "Decoupling the nonlocal elasticity equations for three dimensional vibration analysis of nano-plates", *Compos. Struct.*, **93**, 1015-1020.

Karlicic, D., Murmu, T., Cajic, M., Kozic, P. and Adhikari, S. (2014), "Dynamics of multiple viscoelastic carbon nanotube based nanocomposites with axial magnetic field", *J. Appl. Phys.*, **115**, 234303.

Ke, L. L., Wang, Y.S., Yang, J. and Kitipornchai, S. (2014), "Free vibration of size-dependent magneto-electro-elastic nanoplates based on the nonlocal theory", *Acta Mech. Sinica*, **30**, 516-525.

Kiani, K. (2011a), "Small-scale effect on the vibration of thin nanoplates subjected to a moving nanoparticle via nonlocal continuum theory", *J. Sound Vib.*, **330**, 4896-4914.

Kiani, K. (2011b), “Nonlocal continuum-based modeling of a nanoplate subjected to a moving nanoparticle. Part I: Theoretical formulations”, *Phys. E*, **44**, 229-248.

Kiani, K. (2012a), “Transverse wave propagation in elastically confined single-walled carbon nanotubes subjected to longitudinal magnetic fields using nonlocal elasticity models”, *Phys. E*, **45**, 86-96.

Kiani, K. (2012b), “Magneto-elasto-dynamic analysis of an elastically confined conducting nanowire due to an axial magnetic shock”, *Phys. Lett. A*, **376**, 1679-1685.

Kiani, K. (2012c), “Magneto–thermo–elastic fields caused by an unsteady longitudinal magnetic field in a conducting nanowire accounting for eddy-current loss”, *Mater. Chem. Phys.*, **136**, 589-598.

Kiani, K. (2014a), “Vibration and instability of a single-walled carbon nanotube in a three-dimensional magnetic field”, *J. Phys. Chem. Solid*., **75**, 15-22.

Kiani, K. (2014b), “Elastic wave propagation in magnetically affected double-walled carbon nanotubes”, *Meccanica*, **50**, 1003-1026.

Kiani, K. (2014c), “Longitudinally varying magnetic field influenced transverse vibration of embedded double-walled carbon nanotubes”, *Int. J. Mech. Sci.*, **87**, 179-199.

Kiani, K. (2014d), “Revisiting free transverse vibration of embedded single-layer graphene sheets acted upon by an in-plane magnetic field”, *J. Mech. Sci. Tech.*, **28**, 3511-3516.

Kiani, K. (2014e), “Free vibration of conducting nanoplates exposed to unidirectional in-plane magnetic fields using nonlocal shear deformable plate theories”, *Phys. E*, **57C**, 179-192.

Lee, C.L., Chiou, H.P., Syu, C.M., Liu, C.R., Yang, C.C. and Syu, C.C. (2011), “Displacement triangular Ag/Pd nanoplate as methanol-tolerant electrocatalyst in oxygen reduction reaction”, *Int. J. Hydrogen Energ.*, **36**, 12706-12714.

Li, Y.S., Cai, Z.Y. and Shi, S.Y. (2014), “Buckling and free vibration of magnetoelectroelastic nanoplate based on nonlocal theory”, *Compos. Struct.*, **111**, 522-529.

Malekzadeh, P. and Farajpour, A. (2012), “Axisymmetric free and forced vibrations of initially stressed circular nanoplates embedded in an elastic medium”, *Acta Mech.*, **223**, 2311-2330.

Malekzadeh, P., Setoodeh, A.R. and Alibeygi Beni, A. (2011), “Small scale effect on the free vibration of orthotropic arbitrary straight-sided quadrilateral nanoplates”, *Compos. Struct.*, **93**, 1631-1639.

Mandal, U. and Pradhan, S.C. (2014), “Transverse vibration analysis of single-layered graphene sheet under magneto-thermal environment based on nonlocal plate theory”, *J. Appl. Phys.*, **116**, 164303.

Mindlin, R.D. (1964), “Micro-structure in linear elasticity”, *Arch. Ration. Mech. An.*, **16**, 51-78.

Murmu, T., McCarthy, M.A. and Adhikari, S. (2012), “Vibration response of double-walled carbon nanotubes subjected to an externally applied longitudinal magnetic field: A nonlocal elasticity approach”, *J. Sound Vib.*, **331**, 5069-5086.

Murmu, T., McCarthy, M.A. and Adhikari, S. (2013), “In-plane magnetic field affected transverse vibration of embedded single-layer graphene sheets using equivalent nonlocal elasticity approach”, *Compos. Struct.*, **96**, 57-63.

Murmu, T. and Pradhan, S.C. (2009), “Small-scale effect on the free in-plane vibration of nanoplates by nonlocal continuum model”, *Phys. E*, **41**, 1628-1633.

Narendar, S. and Gopalakrishnan, S. (2012), “Temperature effects on wave propagation in nanoplates”, *Compos. Part B-Eng.*, **43**, 1275-1281.

Narendar, S., Gupta, S.S. and Gopalakrishnan, S. (2012), “Wave propagation in single-walled carbon nanotube under longitudinal magnetic field using nonlocal Euler-Bernoulli beam theory”, *Appl. Math. Modell.*, **36**, 4529-4538.

Pradhan, S.C. and Phadikar, J.K. (2009), “Nonlocal elasticity theory for vibration of nanoplates”, *J. Sound Vib.*, **325**, 206-223.

Sewell, H. (2008), “Method for making a computer hard drive platen using a nano-plate”, U.S. Patent No. 7, 409, 759.

Toupin, R.A. (1964), “Elastic materials with couple stresses”, *Arch. Ration. Mech. An.*, **11**, 385-414.

Wang, H., Dong, K., Men, F., Yan, Y.J. and Wang, X. (2010), “Influences of longitudinal magnetic field on wave propagation in carbon nanotubes embedded in elastic matrix”, *Appl. Math. Model.*, **34**, 878-889.

Wang, Y.Z., Li, F.M. and Kishimoto, K. (2010), “Scale effects on the longitudinal wave propagation in nanoplates”, *Phys. E*, **42**, 1356-1360.

Wang, X., Shen, J.X., Liu, Y., Shen, G.G. and Lu, G. (2012), “Rigorous van der Waals effect on vibration characteristics of multi-walled carbon nanotubes under a transverse magnetic field”, *Appl. Math. Model.*, **36**, 648-656.

Xie, H.J., Wang, X. and Li, Z. (2012), “Dynamic characteristics of multi-walled carbon nanotubes under longitudinal magnetic fields”, *Mech. Adv. Mater. Struct.*, **19**, 568-575.

Zhong, L., Gan, S., Fu, X., Li, F., Han, D., Guo, L. and Niu, L. (2013), “Electrochemically controlled growth of silver nanocrystals on graphene thin film and applications for efficient nonenzymatic H_2O_2 biosensor”, *Electrochim. Acta*, **89**, 222-228.

Zhu, Y., Zhao, Q., Zhang, Y.H. and Wu, G. (2012), “Hydrothermal synthesis of protective coating on magnesium alloy using de-ionized water”, *Surf. Coat. Tech.*, **206**, 2961-2966.

CC